**Manuscript**
**Click here to view linked References**

# Modelling *Zostera marina* and *Ulva spp.* in a coastal lagoon

[1)] Leslie Aveytua-Alcázar, [(1)] Victor F. Camacho-Ibar, [(2)] Alejandro J. Souza, [(3)] J.I. Allen, [(3)] Ricardo Torres.

[(1)] Instituto de Investigaciones Oceanológicas, Universidad Autónoma de Baja California, P.O. Box 453, Ensenada, Baja California 22830, México.

[(2)] Proudman Oceanographic Laboratory, Joseph Proudman Building 6 Brownlow Street Liverpool L3 5DA, UK.

[(3)] Plymouth Marine Laboratory, Prospect Place, Plymouth, Devon, PL1 3DH, UK.

Tel.: +646-1744601, Fax: +646-1745303, laveytua@uabc.mx

## Abstract

We have implemented new modules of seagrass and macroalgae in the European Regional Seas Ecosystem Model (ERSEM). The modules were tested using a version of ERSEM coupled with the General Ocean Turbulence Model (GOTM) in San Quintin Bay (SQB), a coastal lagoon in Baja California, Mexico. As we are working in a region where horizontal advective transport of nutrients is important, we have included the horizontal nutrient gradients which result in nutrient advection when combined with the local currents. The addition of the *Zostera marina* and *Ulva spp*. modules to ERSEM, and the inclusion of advection results in a better simulation of the seasonal and interannual trends in nutrient concentrations and macrophyte biomasses in SQB. The differences between the simulations with and without advection are particularly apparent during the

upwelling periods. Therefore, by increasing the horizontal gradients of nitrate in the model during the strong upwelling seasons a stronger advection results in higher nitrate concentrations from May through July in 2004 and 2005. The difference in the seasonal trend in biomasses between both macrophytes, with *Ulva spp.* reaching its seasonal maximum in June-July and *Z. marina* reaching it in September-October reflects the different response to the various factors controlling their primary production. *Z. marina* is particularly sensitive to variations in the photosynthetically active radiation (PAR) and the light limitation factor, while *Ulva spp.* is more sensitive to changes in the maximum uptake rates of nitrate. The model was forced using field data from the lagoon collected in 2004 and 2005.

Keywords: *Z. marina*, *Ulva spp*., Coastal Lagoon, ERSEM, GOTM, Ecosystem modelling.

## 1. Introduction

Coastal lagoons are characterized by large fluctuations in physical and biogeochemical conditions as a consequence of their location between land and sea (Kjerfve 1994). Coastal lagoons are relatively shallow and tend to be dominated by benthic primary producers, such as seagrass, macroalgae and benthic microalgae rather than by phytoplankton (Tyler et al. 2001). This promotes a strong benthic-pelagic coupling that influences carbon and nutrient dynamics, as well various aerobic and anaerobic respiration pathways. Like

47 estuaries, coastal lagoons represent environments with high productivity (Pauly
48 and Yañez-Arancibia 1994).

49 Coupled hydrodynamic-ecosystem models are tools to assess the major
50 qualitative aspects of the ecosystem and help in addressing important issues for
51 coastal zone management (Torres et al. 2006). Marine ecosystem models
52 describing the geochemical and biological cycling have been developed for many
53 regions particularly during the last 10 years. One of the most complex marine
54 ecosystem models developed to date is the European Regional Seas Ecosystem
55 Model (ERSEM; Baretta-Bekker et al. 1995). Originally developed as a box
56 model describing biogeochemical cycling within the North Sea, ERSEM has
57 nowadays been successfully adapted to other ecosystems. For example, Allen et
58 al. (1998) used the model in the Adriatic Sea to contrast the ecosystem
59 functionality. Blackford and Burkill (2002) have applied ERSEM in the Arabian
60 Sea, to explore the differences between monsoonal waters and unperturbed
61 oligotrophics oceanic sites, while Vichi et al. (1998) used the model on seasonal
62 response in shallow Northern Adriatic. In this study, we have used ERSEM
63 coupled with the General Ocean Turbulence Model (GOTM), a 1-DV numerical
64 model with several modern turbulence closure schemes, which has become the
65 community workhorse, to simulate the physical and biogeochemical processes in
66 San Quintin Bay (SQB). For the model to be able to correctly represent SQB
67 biogeochemistry, newly developed seagrass and macroalga modules had to be
68 included.

SQB is a coastal lagoon (Figure 1) located in the coast of Baja California, Mexico (30°27'N, 116°00'W), covering an area of ~ 42 $km^2$ with an average depth of 2 m, a maximum tidal amplitude of 2.4 m during spring tides, and water temperature ranges of 11-22 °C and 13-27 °C at the m outh of the bay and at the inner end of the eastern arm, respectively (Alvarez-Borrego and Alvarez-Borrego 1982). San Quintin is a Mediterranean-type coastal lagoon (Largier et al. 1997), and is a hypersaline system throughout year (Camacho-Ibar et al. 2007). This temperate region of the Baja California Peninsula has a mean annual precipitation of 150 mm and a mean annual evaporation of 1400 mm; rainfall is restricted to the period of November to March. As evidenced by saline intrusion, over extraction of groundwater for agriculture has induced a reversal of the groundwater flow in the coastal aquifers, making them an unlikely source of nutrients to the bay (Aguirre-Muñoz et al. 2001). Most of the inhabitants of the catchment, which is a rural area, live away from shore. Tourism, which is one of the main economic activities in the locality, is still limited and represents a minor indirect source of nutrients to the bay.

SQB ecology is strongly influenced by the presence of extensive meadows of the eelgrass *Zostera marina* (Ward et al. 2003; Jorgensen et al. 2007). Ward et al. (2003) indicate that this species covers ~40% of this lagoon, and is dispersed throughout the Bay, forming particularly dense patches at the inner arms. Large mats of *Ulva spp.* are mainly concentrated in Bahia Falsa and also near the mouth of the bay. Although *Ulva spp*. is present all year around, its biomass shows a seasonal variation with a spring maximum. Biomasses of 1400

92 dry t were measuredt during spring (May) 2004 and 1160 dry t in early summer
93 (June) 2005, distributed in an area of 431 and 303 ha, respectively. In winter
94 2004 Ulva biomass reached only 35 dry t in an area of 54 ha (Zertuche-
95 González, pers. comm., 2008).

96 The Pacific oyster *Crassostrea gigas* has been cultivated commercially in
97 the western arm of the lagoon (Bahia Falsa) since the late 70's (García-Esquivel
98 et al. 2004), and represents a functional group that may be explicitly included in
99 the SQB ecosystem model.

100 The main external physical and biogeochemical forcing in this lagoon is
101 from the neighbouring coastal ocean, strongly influenced by upwelling. Although
102 wind conditions may induce upwelling events throughout the year in this area, the
103 most intense upwelling occurs during spring and early summer (Bakun and
104 Nelson 1977). Upwelling pulses advect water into SQB, supplying new nitrogen
105 (nitrate), which is rapidly taken-up and promotes high phytoplankton, macroalgae
106 and seagrass productivity and biomass within the bay (Camacho-Ibar et al.
107 2007). The frequency of the upwelling pulses likely controls the temporal
108 variability of primary production and nutrients at the bay's mouth (Lara-Lara et al.
109 1980).

110

111 **2. Description of the modelling system**

112 To better understand the physical-biogeochemical interactions it was
113 decided to use a one-dimensional vertical framework to combine the best
114 hydrodynamic model of this kind (GOTM) and one of the most complete

ecological models available (ERSEM). A two way coupling between water column and biogeochemistry is applied. The dependence of the biogeochemistry on the physics is established via vertical mixing and horizontal advection of nutrients, temperature and salinity, light availability and many other mechanisms. The advantage of using a 1-DV framework is that the hydrodynamics is kept as simple as possible, while still maintaining the necessary physical processes, in such way that we can focus on studying the importance of the newly incorporated functional groups (i.e. *Z. marina* and *Ulva spp.*).

## 2.1 Physical model

A one-dimensional numerical model for the water column is applied here, consisting of prognostic equations for horizontal velocity components, temperature and salinity. Density is calculated by means of UNESCO equation of state (http://fermi.jhuapl.edu/denscalc.html) as function of temperature and salinity and hydrostatic pressure. The model is externally forced by $M_2$ and $S_2$ barotropic tidal currents derived from observations, and wind stress, surface heat and momentum fluxes, calculated by bulk formulae using atmospheric measurements. A detailed description of the numerical model is given by Bolding et al. (2002) and references therein (see http://www.gotm.net).

A k-ε turbulence closure scheme is used here, where the turbulent dissipation rate is discussed in detail in Canuto et al. (2001) and Umlauf and Burchard (2005). The stability functions used here are those suggested by Canuto et al. (2001).

Although advection of momentum has not been considered in the model, the horizontal velocities combined with horizontal nutrient gradients are used to calculate the horizontal advection of nutrients and in that way incorporate the advection of newly upwelled nutrients from the ocean.

## 2.2 The ecological model

The European Regional Seas Ecosystem Model was developed by a number of scientists at several institutes across Europe through projects under the MAST Programme of the European Union. Many features and applications of the ERSEM model are described in Baretta et al. (1995) and Baretta-Bekker and Baretta (1997).

ERSEM is a modelling framework in which the ecosystem is represented as a network of physical, chemical and biological processes. It uses a ‘functional group’ approach to describe the ecosystem, whereby biota are grouped together according to their trophic level and sub-divided according to size and feeding method. The ecosystem is subdivided into three functional group types: primary producers, consumers and decomposers. Physiological (ingestion, respiration, excretion and egestion) and population (growth, and mortality) processes are included in the descriptions of functional group dynamics. These dynamics are described by fluxes of carbon and nutrients between functional groups. Each functional group is defined by a number of components, namely carbon (C), nitrogen (N), and phosphorus (P) and, in the case of diatoms, silicate (Si), each of which is explicitly modelled. The phytoplankton pool is described by four

functional groups. These are diatoms, flagellates, picoplankton and nanoplankton. All phytoplankton groups contain internal nutrient pools and have dynamically varying C:N:P ratios. The nutrient uptake is controlled by the difference between the internal nutrient pool and external nutrient concentration. The microbial loop contains bacteria, mesozooplankton and microzooplankton each with dynamically varying C:N:P ratios.

The benthic sub-model contains a food web which describes nutrient and carbon cycling via both aerobic and anaerobic bacterial pathways, bioturbation/bioirrigation and the vertical transport in sediment of particulate matter is due to the activity of benthic biota. The benthic nutrient model treats N, P and Si, and their exchange with the pelagic system depending on the nutrient gradients at the sediments surface. The mineralization of organic matter, coupled to diagenetic nutrient processes in the sediments, is also included in the sub-model (Ruardij and van Raaphorst 1995). Detailed descriptions of ERSEM can be found in Baretta et al. (1995); Baretta-Bekker et al. (1995, 1997), Blackford (1997), Ebenhoh et al. (1995). Full ERSEM model equations can be found at http://www.pml.ac.uk/ecomodels/ersem.html.

In an attempt to realistically simulate nutrient dynamics in the SQB ecosystem, the food web with the trophic relationships among the different groups was set up as shown in Figure 2. State variables of *Z. marina* and *Ulva spp.* are included (Table 1) to simulate the seasonal dynamics of their biomass.

**2.3 Seagrass module**

184 The *Z. marina* module is conceptually similar to the phytoplankton module
185 in ERSEM, and is based on the *Z. marina* model proposed by Bocci et al. (1997).
186 Seagrasses take nutrients from sediments through roots and rhizomes, and from
187 the water column through their shoots. Therefore, the seagrass module includes
188 a shoot sub-module which connects with the pelagic sub-model and a (rhizome-)
189 root sub-module which connects with the benthic sub-model. Both sub-models
190 exchange nutrients through a translocation routine.

191 State variables included in the module are: leaf biomass (S1) and root
192 biomass (S2). The rate of change of total biomass for *Z. marina* (S) is given by
193 the combination of four processes. Production (pS), respiration (rS), exudation
194 (eS) and mortality (morS):

195 $$\frac{\mathbf{dS}}{\mathbf{dt}} = \mathbf{(pS - rS - eS - morS)}$$

196 Light and temperature control seagrass photosynthesis. The gross
197 production rate (pS) was then calculated by maximum growth rate ($\mu_{max}$),
198 modified by temperature ($f_t$), light ($f_i$) and nutrient limitation ($f_N$) factors:

199 $$\mathbf{pS} = \boldsymbol{\mu}_{\mathbf{max}} \mathbf{* f_t * f_i} * f_N$$

200 The dependence on water temperature (T) is common to all the
201 parameterizations of the functional groups and of many other biogeochemical
202 processes in ERSEM. It is written in an exponential form as:

203 $$\mathbf{f_t} = \mathbf{q_{10}^{0.1*(T-10)}}$$

204 where $q_{10}$ is a temperature coefficient.

The light factor ($f_i$) is a function of the extinction coefficient (xeps), water depth (z), and daily total radiation. The total radiation was calculated from the ratio of the superficial (PIo) and depth irradiance (PIz). Plo (the irradiance just below the water surface) is the astronomical irradiance reduced by loss factors: cloud cover, absorption and reflection on the water surface (Ebenhoh et al. 1997). The photosynthetically active radiation (PAR) was multiplied by a conversion factor (fPAR) in order to calculate superficial irradiance.

The extinction coefficient was calculated as a function of the background extinction of water, and extinction due to phytoplankton, particulate detritus and suspended inorganic matter. PKi is the photosynthesis half saturation constant.

$$\mathbf{PIo} = \mathbf{PAR} * \mathbf{fPAR}$$

$$\mathbf{PIz} = \mathbf{PIo} * \mathbf{exp}(-\mathbf{xeps} * \mathbf{z})$$

$$\mathbf{f_i} = \mathbf{tanh}\left(\frac{\mathbf{PIz}}{\mathbf{pK_i}}\right)$$

Self shading effect is not included in the model, as we assume that the plant length (typically < 0.6 m) is smaller than the average water depth in SQB (~ 2 m), allowing leaves to float erect and reduce self-shading.

Fouling on seagrass leaves has been reported as an important control on light availability, and thus on seagrass production, in eutrophic systems (Borowitzka et al. 2006). This has lead to efforts to explicitly include epiphytic algae in seagrass models (Plus et al. 2003; Dixon 2004). However, we have not included ephiphytic algae in our current *Z. marina* module since Jorgensen et al. (2007) reported that, in SQB, neither eelgrass shoot nor aboveground biomass

were related to the epiphyte biomass over eelgrass leaves. These authors reported relatively low epiphyte biomass on eelgrass leaves near the mouth of the lagoon, emphasizing a top-down control of epiphytes, despite high nutrient availability (Jorgensen et al. 2007).

The respiration rate (rS) is a function of the sum of the active respiration (ract) and the basal respiration (rrest) rates, and the plant biomass. The active respiration rate is proportional to pS by a respiration coefficient (pu_raS). The basal respiration rate is a function of seawater temperature and a respiration coefficient (pu_reS).

$$\mathbf{rS} = \mathbf{(rrest} + \mathbf{ract)} * \mathbf{S}$$

$$\mathbf{ract} = \mathbf{pS} * \mathbf{(pu\_raS)}$$

$$\mathbf{rrest} = \mathbf{f_t} * \mathbf{(pu\_reS)}$$

The exudation process (eS) is a function of an exudation coefficient (pu_eaS) t and the gross production rate:

$$\mathbf{eS} = \mathbf{pS} * \mathbf{(pu\_eaS)}$$

Mortality is defined by a temperature factor ($f_t$), a mortality coefficient (pu_daS) related to tissue senescence, and seagrass biomass:

$$\mathbf{morS} = \mathbf{pu\_daS} * \mathbf{f_t} * \mathbf{S}$$

The rates of dissolved and particulate organic matter production in the *Z. marina* module (fSR1 and fSR6, respectively) are a function of an exudation rate and mortality. The carbon fraction to particulate organic matter is defined by a parameter that is the nitrogen and phosphorus fractions, determined by the

minimal nitrogen/carbon and phosphorus/carbon quota. The organic matter produced in this module is transferred into the dissolved (R1) and particulate (R6) organic matter pools in the pelagic sub-model:

$$\mathbf{fSR6} = \mathbf{morS}$$

$$\mathbf{fSR1} = \mathbf{eS} * \mathbf{S}$$

The model considers *Z. marina* growth to be a function of the external nutrient concentration and the nutrient content of the cell, i.e., the internal quota relative to its upper and lower limits according to the kinetics described by Droop (1973). Leaves can consume both nitrate (N3) and ammonium (N4) while, for the roots, only ammonium uptake is considered, because of the prevalence of this form of nitrogen in the sediments. The internal nitrate and ammonium concentration in *Z. marina* N(3,4) and the phosphate (P) concentration is calculated according to a set of differential equations:

$$\frac{\mathbf{dN(3,4)}}{\mathbf{dt}} = \mathbf{uptake} - \boldsymbol{\mu}_{\mathbf{max}} * \mathbf{N(3,4)}$$

$$\frac{\mathbf{dP}}{\mathbf{dt}} = \mathbf{uptake} - \boldsymbol{\mu}_{\mathbf{max}} * \mathbf{P}$$

$$\mathbf{uptake} = (\mathbf{uptakeS1} + \mathbf{uptakeS2}) * \mathbf{f(N3,4)}$$

$$\mathbf{uptakeS1} = \mathbf{uptakeS1}_{\mathbf{N4}} + \mathbf{uptakeS1}_{\mathbf{N3}}$$

$$\mathbf{uptakeS2} = \mathbf{uptakeS2}_{\mathbf{N4}}$$

In the model, nutrient uptake rates are proportional to nutrient concentration in the water column according to Michaelis-Menten kinetics. $UptakeS1_{N4}$, $uptakeS1_{N3}$ and $uptakeS2_{N4}$ are, respectively, the uptake rates for

ammonium and nitrate by the shoots and the uptake rate of ammonium by the roots. $KS1_{N4}$, $KS1_{N3}$ and $KS2_{N4}$ are the half-saturation coefficients in the water column (w) and the sediments (s), and $VmS1_{N4}$, $VmS1_{N3}$ and $VmS2_{N4}$, are the maximum uptake rates of nutrients:

$$\mathbf{uptakeS1_{N4}} = \mathbf{VmS1_{N4}} \frac{\mathbf{[N4w]}}{\mathbf{[N4w]} + \mathbf{KS1_{N4}}}$$

$$\mathbf{uptakeS1_{N3}} = \mathbf{VmS1_{N3}} \frac{\mathbf{[N3w]}}{\mathbf{[N3w]} + \mathbf{KS1_{N3}}}$$

$$\mathbf{uptakeS2_{N4}} = \mathbf{VmS2_{N4}} \frac{\mathbf{[N4s]}}{\mathbf{[N4s]} + \mathbf{KS2_{N4}}}$$

The range of internal nitrogen concentration is controlled by applying a feedback effect to the uptake functions:

$$\mathbf{fN(3,4)} = \frac{\mathbf{N(3,4)max} - \mathbf{N(3,4)}}{\mathbf{N(3,4)max} - \mathbf{N(3,4)min}}$$

In the current version of the model, if the external nutrient concentration is high, the internal N concentration may reach its maximum, causing uptake to cease (i.e., luxury N uptake and storage are not included in the model). Details of the effect of the feedback function on nutrient uptake are given in Bocci et al. (1997).

### 2.4 Macroalgae module

The implementation of *Ulva spp.* module is conceptually similar to the *Ulva rigida* model of Solidoro et al. (1997).

289 The biomass of *Ulva spp*. is considered to be governed by the following
290 processes: production (pU), respiration (rU), exudation (eU) and mortality
291 (morU*).* The general differential equation for biomass (U, expressed as g DW $m^{-2}$
292 ) which includes these processes is:

293 $$\frac{dU}{dt} = (pU - rU - eU - morU)$$

294

295 The gross production rate (pU) is a function of the maximum growth rate
296 ($\mu_{max}$, expressed in $time^{-1}$), modified by temperature ($f_t$), light ($f_i$) and nutrient
297 limitation ($f_N$) factors:

298 $$pU = \mu_{max} * f_t * f_i * f_N$$

299 The temperature and irradiance functions are similar to those in the *Z.*
300 *marina* module. The nutrient limitation factor employs “Droop kinetics” (Droop,
301 1973). The nitrogen and phosphorus concentrations in *Ulva spp.* are calculated
302 like in *Z. marina* module:

303 $$\frac{dN(3,4)}{dt} = uptakeU_{N4} + uptakeU_{N3} - \mu_{max} * N(3,4)$$

304 $$\frac{dP}{dt} = uptakeU_{P} - \mu_{max} * P$$

305 The range of internal nutrient concentration is controlled by applying a feedback
306 effect to the uptake functions:

307 $$fP = \frac{Pmax - P}{Pmax - Pmin}$$

308 The nutrient limitation function assumes that *Ulva spp*. growth is 0 when the
309 simulated internal quota equals the minimal internal quota:

310 $$f_P = 1 - \frac{Pmin}{P}$$

311

312 **3. Model application area, initial conditions and forcing**

313 The simulation period in this study corresponds to January 2004 to
314 October 2005 (beginning after a 1-year period initialization), a period which
315 includes two seasons of upwelling intensification in April-June each year. Due to
316 the one-dimensional character of GOTM, most of the state variables are
317 assumed to be horizontally homogeneous, depending only of the vertical z-
318 coordinate. The model is forced by local $M_2$ and $S_2$ along channel tidal currents
319 derived from an RDI acoustic Doppler current profiler (ADCP) located near the
320 mouth of SQB (Figure 1). As the long axis of the channel at the mouth of the bay
321 where currents were measured is aligned in a north-south direction, and the
322 station of simulation is orientated to – 45° of the main channel, measured tidal
323 velocities were re-oriented. The physical model was forced with daily
324 observations with a meteorological station of wind velocity, irradiance, air
325 temperature and atmospheric pressure from the period 2004 (Figure 3) and 2005
326 (data not shown). The model was initialized with January 2004 temperature and
327 salinity values. Some of the biogeochemical parameters in the ecosystem model
328 are based on *in situ* observations during field campaigns in spring and summer of
329 2004, spring 2005 and summer 2003 (e.g., Table 2 and 3). Due to the lack of
330 field information, all other parameters are the standard ERSEM values. This

appears to be a robust approximation, as demonstrated by Blackford et al. (2004) for a range of coastal environments, including coastal lagoons (Petihakis et al. 1999).

For the initialization of the model and due to the lack of data for the seasonality of nutrients in SQB throughout the whole year, it was assumed that winter nutrient concentrations are similar to values observed during mid-intensity upwelling (6 μM for nitrate, 4 μM for ammonium, 2 μM for phosphorus and 15 μM for silicate). Experimental and literature data were used to parameterize the scalars for each functional group. Some parameters that were not measured (e.g. growth rates) were estimated and adjusted to better fit of the model (Table 2 and 3). The initial biomass was set to 60 g DW $m^{-2}$ both for *Z. marina* and *Ulva spp.*

The station chosen for the simulations is located 2 km from the mouth of the bay (Figure 1). Nutrient concentration gradients used for the simulations (Figure 4) were assumed to follow a seasonal cycle based on upwelling intensity (see Pennington and Chavez 2000). The values used during the season of upwelling intensification are within the higher range of our observations calculated from the difference in nutrient concentrations at adjacent sampling stations (Figure 1). Upwelling in the spring 2005 was more intense in comparison to 2004, thus nitrate gradients with which the model was forced were larger in 2005 (Figure 4). It was assumed that nutrient gradients during winter, where no observations are available, are small as biological activity in this season is usually low and horizontal mixing may prevail.

## 4. Sensitivity analysis

To examine the influence of individual parameters and processes on nutrient concentrations and primary producers biomass, a sensitivity analysis was performed. We have chosen parameters related to light and nutrient availability which are the controlling factors on primary production in this ecosystem. Sensitivity analysis has been done varying photosynthetically active radiation (PAR), the light limitation factor, and the maximum uptake rates of nitrate ($VmS1_{N3}$ and $VmU_{N3}$). Variations of + 30 and - 30% around the standard simulation have been applied to each parameter. In the case of PAR, the standard value used in the model is 50 W $m^{-2}$ (~ 15 mol quanta $m^{-2}$ $d^{-1}$ reported by Cabello-Pasini et al. 2003). In the case of the light limitation factor, a dimensionless factor which depends on the light extinction coefficient (~1.1 $m^{-1}$ for SQB; Cabello-Pasini et al. 2003) and the light fraction of the day (~ 0.5, 12 h), the standard value used is 0.68. The light limitation factor is ~ 3*light fraction day/extinction coefficient *depth (Ebenhöh et al. 1997). The standard uptake rate value for *Z. marina* ($VmS_{N3}$) is 0.06 mg g $DW^{-1}$ $h^{-1}$ (Bocci et al. 1997) and the standard value for *Ulva spp.* ($VmU_{N3}$) is 0.7 mg g $DW^{-1}$ $h^{-1}$ (Guimaraens et al. 2005).

## 5. Results and discussion

In order to model nutrient dynamics in shallow coastal ecosystems such as estuaries and coastal lagoons, where macrophytes contribute significantly to

primary production, complex ecosystem models are required. ERSEM is a complex model originally developed and validated for shelf waters (Baretta et al. 1995; Allen et al. 1998; Blackford y Burkill 2002) which has also been applied in one coastal lagoon, Gialova lagoon (Petihakis et al. 1999). In the latter case, ERSEM was simplified by reducing the number of original state variables and keeping phytoplankton as the only primary producers. In our study, in order to realistically simulate nutrient dynamics in SQB, newly developed seagrass and macroalgae modules had to be included. To validate the inclusion of these modules, and given the strong horizontal nutrient gradients induced in SQB by upwelling events, GOTM had to include advection of nutrients.

The inclusion of advection in GOTM results in higher nutrient concentrations in the simulations (Figure 5). The differences between the simulations with and without advection are particularly apparent during the upwelling periods where both nitrate and ammonium show a better fit to field data (Figure 5). Although the seasonal increase in nitrate concentrations during both upwelling periods results from the increased concentration gradient (Figure 4), the peaks during such periods are likely caused by oscillations in phytoplankton biomass (Figure 6).

Adding advection to GOTM also results in higher biomass of all primary producers, leading to reported literature values of *Z. marina*, *Ulva spp.* and diatoms (Figure 6). Without advection, the maximum foliar biomass of *Z. marina* during summer-autumn is 100 g DW $m^{-2}$ during both years. While the maximum of 2004 (110 g DW $m^{-2}$) with advection is only 10% higher that without advection,

400 the maximum of 2005 is ~ 50% higher that the biomass without advection. Ibarra-
401 Obando et al. (2007) reported an average annual foliar biomass in SQB of 75 g
402 DW $m^{-2}$, with annual maxima ranging from ~ 80 to ~ 350 g DW $m^{-2}$, and an
403 average in the summer-autumn maxima of ~ 150 g DW $m^{-2}$. In the case of *Ulva*
404 *spp.*, without advection the early-summer maximum is similar in 2004 and 2005,
405 with a value of ~ 80 g DW $m^{-2}$, and when advection is included maxima are 120
406 and 130 g DW $m^{-2}$ respectively. Zertuche-González (pers. comm., 2008) report
407 biomasses ~ 350 g DW $m^{-2}$ within *Ulva spp.* beds near our simulation station in
408 SQB in spring-summer 2004 and 2005, and ~ 65 g DW $m^{-2}$ in late winter 2005.
409 As biomasses reported by these authors are for *Ulva spp.* beds (i.e. a site with
410 100% cover by this macrophyte), their values should be considered an upper
411 limit for biomasses expected at our simulation site where *Ulva spp.* and *Z. marina*
412 co-exist. Without advection, spring diatom blooms are essentially absent in our
413 runs while several blooms appear, with particularly high intensity, in May and
414 June when advection is added. Maximum diatom biomasses of 250 - 300 mg C
415 $m^{-3}$ are consistent with biomasses of ~ 240 mg C $m^{-3}$ estimated from chlorophyll
416 a measurements (~ 4 mg Chla $m^{-3}$) reported by Millan-Nuñez et al. (1982) for
417 June-July.

418 The addition of nutrient advection also results in a better simulation of the
419 seasonal and interannual trends in nutrient concentrations and macrophyte
420 biomasses in SQB. During the strong upwelling season (April-June), horizontal
421 nutrient (particularly nitrate) gradients increase as a result of increased nutrient
422 concentrations at the oceanic end due to the advection of upwelled waters

(Camacho-Ibar et al. 2007). Therefore, by increasing the horizontal gradients of nitrate in the model during the strong upwelling seasons a stronger advection results in higher nitrate concentrations from May through July in 2004 and 2005 (Figure 5). However, in spite of the increase in nutrient concentration with the inclusion of advection, the simulated values during the upwelling periods are below the concentrations measured in field samples. This difference between modelled and observed values is more apparent for nitrate in 2005, when stronger upwelling in the region promoted higher nitrate concentrations (up to 14 μM) at the modelled site. This discrepancy is mostly due to the consumption of nitrate by *Ulva spp.* as indicated by the maximum nitrate concentration (~ 10.5 μM) observed in the simulation when the *Ulva spp.* module is switched-off (Figure 5).

The difference in the seasonal trend in biomasses between both macrophytes, with *Ulva spp.* reaching its seasonal maximum in June-July and *Z. marina* reaching it in September-October reflects the different response to the various factors controlling their primary production. In the case of seagrasses, production is frequently regulated by underwater irradiance, temperature and environmental nutrient availability (Dennison and Alberte 1982; Trancoso et al. 2005), with underwater light availability being usually the most important controlling factor (Zimmerman et al. 1987; Cabello-Pasini et al. 2003). By contrast, *Ulva spp.* production is usually regulated by nitrogen availability and, therefore, uptake rates (Burd and Dunton 2001; Guimaraens et al. 2005).

445 The seasonal evolution of *Z. marina* foliar biomass in our simulations, as
446 expected, shows a maximum in late summer and early autumn of 150 g dry w $m^{-2}$
447, when seawater temperature is maxima, and decreases to ~ 70 g dry w $m^{-2}$ in
448 winter and early spring. The rapid increase in biomass occurs in June-July
449 (Figure 6) when light irradiance is at its peak (Figure 3). This is a similar pattern
450 to the one described for eelgrass in SQB (Poumian-Tapia and Ibarra-Obando
451 1999; Cabello-Pasini et al. 2003; Ibarra-Obando et al. 2007). The interannual
452 difference in our simulations, with higher biomasses observed in 2005, is not due
453 to a difference in irradiance but it is likely due to the increased availability of
454 nitrate. Ibarra-Obando et al. (2007) speculate that the large interannual variability
455 in foliar biomass they observed in *Z. marina* in SQB, were associated with
456 variations in nutrient availability. ERSEM-GOTM simulations result in a seasonal
457 cycle of the *Ulva spp.* biomass, with values starting to increase in May, reaching
458 maxima of 130 g dry w C $m^{-2}$ in June-July, and rapidly decreasing by 50 % from
459 September through April in response to relatively low nitrate availability (Figure
460 6). *Ulva spp.* is generally sparse in winter and early spring when its growth is
461 likely limited by environmental factors such as light and temperature. The
462 interannual variation in maximum *Ulva spp.* biomass induced by higher nitrate
463 concentrations in the model agree with the observations by Zertuche-González
464 (pers. comm., 2008) who report higher densities in *Ulva spp.* beds and higher
465 nitrogen content in the plants in June 2005 as compared to May 2004.
466 Simulated biomasses in our model are particularly sensitive to light related
467 parameters (PAR and light limitation factor) in the case of *Z. marina*, and to

maximum nitrate uptake rate variations in the case of *Ulva spp.* We hypothesized that in SQB water temperature, compared with light, has only a minor control on the seasonal patterns of *Z. marina* (and *Ulva spp.*) biomass, as optimal temperature for *Z. marina* growth has been reported between 15 and 20 ℃ (Kaldy and Lee 2007), a temperature range typical for the seasonal variation in mean daily temperature near the mouth within SQB (data not shown). Cabello-Pasini et al. (2003) estimated the annual variations of *Z. marina* biomass at three coastal lagoons in Baja California, Mexico, and concluded that irradiance is the most important factor controlling annual variations of biomass and distribution of this seagrass. Kaldy and Lee (2007) reported that temperature is not an important factor controlling seasonal variations in *Z. marina* biomass in Yaquina Bay, Oregon, an estuarine system in the California Current also influenced by coastal upwelling, where temperature ranges from 9 to 13 ℃.

In our sensitivity analysis, variations in PAR by ± 30% produce concomitant changes in foliar *Z. marina* biomass which are more apparent in both maxima (~ 20 - 25 g DW $m^{-2}$). *Ulva spp.* also responds to variations in PAR, although its changes (< 10 g DW $m^{-2}$) are smaller than for *Z. marina* (Figure 7). The higher sensitivity of *Z. marina* to light changes is also evident when the light limitation factor is varied (Figure 8). Whereas foliar *Z. marina* biomass varies ~ 15 – 20 g DW $m^{-2}$ with a ± 30% variation in the light limitation factor (biomass increases as light extinction decreases), *Ulva spp.* biomass changes ~ 10 g DW $m^{-2}$ (Figure 8).

Understanding and predicting through modelling the effect of changes of light availability on *Z. marina* communities is important to understanding the SQB ecosystem. The annual variation of the biomass and photosynthesis of *Z. marina* in three coastal lagoons along the coast of Baja California, including SQB, have been related to differences in irradiance, water clarity and temperature (Cabello-Pasini et al. 2003). In general there is an increase of the levels of irradiance and of the annual variation in temperature in the lagoons to the south of SQB. The smaller availability of light in SQB causes a latitudinal difference in the spatial distribution of *Z. marina*, with an increase in biomasses of intertidal meadows in this lagoon (Cabello-Pasini et al. 2003) as seagrass depth limits are strongly related to the underwater light penetration and light extinction (Duarte et al. 2007). This distribution makes SQB seagrass meadows particularly sensitive to natural and human induced changes in water quality. Ward et al. (2003) reported a 34% loss of subtidal seagrass coverage over a 13-yr period apparently due to an increase in water turbidity, whereas only a 13% gain was observed in intertidal areas. If urban areas and tourism increase around the bay, water clarity issues can be a threat to *Z. marina* communities. For example, sediment transported from cleared land to coastal water can indirectly damage seagrass by blocking out the light that it needs to grow. Phytoplankton and epiphytic macroalgae are a common result of excess nutrients delivered to coastal waters; increased amounts of these producers may remove a large percentage of the light that would otherwise have been available for seagrass photosynthesis (Ralph et al. 2006).

513 In contrast to the seagrass, in our model *Ulva spp.* is less sensitive to light
514 availability and more sensitive to nitrogen availability as is frequently the case in
515 upwelling influenced coastal ecosystems (Guimaraens et al. 2005). The 30%
516 variation in the maximum uptake rate of nitrate (i.e. nitrate consumption by the
517 plant) results in a variation ~ 10 g DW $m^{-2}$ of *Z. marina* shoot biomass and a
518 variation ~ 25 – 35 g DW $m^{-2}$ of *Ulva spp*. (Figure 9). Although nitrogen is
519 generally considered the most limiting nutrient to eelgrass, seagrasses can take
520 nitrogen (especially ammonium) and phosphorus from sediment pore water and
521 the water column (mostly nitrate) (Kaldy and Lee 2007). The importance of
522 leaves versus roots uptake depends, in part, on nutrient concentrations in the
523 water column. In SQB concentrations of interstitial ammonium are typically > 200
524 μM (unpublished data), a value well above the suggested threshold concentration
525 for nitrogen limitation for seagrass growth (Lee and Dunton 2000). However, our
526 sensitivity analysis supports the previous suggestion that interannual variability in
527 foliar biomass in *Z. marina* observed in our simulations are associated with
528 variations in nitrate availability/consumption as has been suggested for SQB
529 (Ibarra-Obando et al. 2007).

530 The larger sensitivity of *Ulva spp.* biomass to nitrate uptake in our
531 simulations for SQB (i.e. *Ulva spp*. biomass changes ~ 30% with a 30% variation
532 in the maximum uptake rate whereas *Z. marina* biomass only varies ~ 10%), is
533 consistent with macroalgae models for other coastal systems (Guimaraens et al.
534 2005, Trancoso et al. 2005). In a modelling study of macroalgae in a shallow
535 temperate coastal lagoon, Trancoso et al. (2005) indicate that nitrogen

536 availability in the system is the most important limiting factor of macroalgae
537 growth. In turn, their modelling results show a significant control of macroalgae
538 on dissolved nitrogen concentrations. This was also observed in our study, where
539 without *Ulva spp*. nitrate concentrations in the water column increased by ~ 4 µM
540 (Figure 5). This is a substantial variation considering the ~ 3 µM mean annual
541 nitrate concentration at our modelling site. This higher sensitivity of *Ulva spp*. to
542 nitrogen uptake is also consistent with the spatial distribution of *Ulva spp*. carbon
543 stocks within SQB, as higher densities and larger beds are observed near the
544 mouth of the lagoon where the influence of nitrate supply from the ocean is larger
545 than at the inner ends (Camacho-Ibar et al. 2007). The larger biomass of Ulva
546 toward the south of the lagoon may additionally be explained by the
547 accumulation of floating beds due to the action of NW dominant winds which
548 induce residual surface currents towards the SE (Flores-Vidal 2006).
549

550 **6. Conclusion**

551 Our results show that the advection of nutrients added to GOTM
552 significantly improved the simulation of the seasonal nutrient concentrations, and
553 *Ulva spp.* and *Z. marina* biomasses in SQB, an upwelling influenced coastal
554 ecosystem.

555 The addition of the *Z. marina* and *Ulva spp*. modules to ERSEM, a
556 complex ecosystem model, allowed for the representation of seasonal trends of
557 the biomasses of these macrophytes. However, field data are required to validate
558 the magnitudes of biomasses which may show intense interannual variations. *Z.*

559 *marina* is particularly sensitive to PAR and the light limitation factor whereas *Ulva*
560 *spp*. is more sensitive to the maximum uptake rates of nitrate. Consequently, for
561 a better estimation of seasonal variation of *Ulva spp*. biomass in SQB, a
562 calibration of maximum uptake rates of nitrate is required. In order to simulate
563 more realistically the dynamics of *Z. marina* and *Ulva spp.* biomass in SQB and
564 other shallow coastal ecosystems, factors such as shoot loss due to wave action,
565 grazing, self shading and epiphyte fouling, have to be included in the model.
566

567 **Acknowledgments**

568 This work was supported by SEP-CONACyT-México (grant No. 40144) to
569 VCI. Grants from CONACyT (No. 144066), UABC and POGO provided to LAA
570 are acknowledged. We thank to UABC personnel for assistance with laboratory
571 and field work, and to personnel from POL and PML for assistance on modelling.
572

573 **References**

574 Aguirre-Muñoz, A.R., Buddemeir, W., Camacho-Ibar, V.F., Carriquiry, J.D.,
575 Ibarra-Obando, S.E., Mass, B., Smith, S.V., Wulff, F., 2001. Sustainability of
576 coastal resources in San Quintin, Mexico. Ambio, 30, 142-149.

577 Allen, J.I., Blackford, J.C., Radford, P.J., 1998. A 1-D vertically resolved
578 modelling study of ecosystem dynamics of the middle and southern Adriatic Sea.
579 Journal of Marine Systems, 18, 265-286.

580 Álvarez-Borrego, J., Álvarez-Borrego, S., 1982. Temporal and spatial variability
581 of temperature in two coastal lagoons. CalCOFI Reports XXIII, 188-197.

582 Bakun, A., Nelson, C.S., 1977. Climatology of upwelling related processes off
583 Baja California. CalCOFI Reports, 19, 107-127.
584 Baretta, J.W., Ebenhöh, W., Ruardij, P., 1995. The European Regional Seas
585 Ecosystem Model (ERSEM), a complex marine ecosystem model. Netherlands
586 Journal of Sea Research, 33 (3/4), 233-246.
587 Baretta-Bekker, J., Baretta, J., W., Rasmussen, E., 1995. The microbial food web
588 in the European Regional Seas Ecosystem Model. Netherlands Journal of Sea
589 Research, 33, 233-246.
590 Baretta-Bekker, J.G., Baretta, J.W., 1997. Preface to the European Regional
591 Seas Ecosystem Model (ERSEM ll). Journal of Sea Research, 38 (3/4), 169-170.
592 Baretta-Bekker, J., Baretta, J.W., Ebenhöh, W., 1997. Microbial dynamics in the
593 marine ecosystem model ERSEM II with decoupled carbon assimilation and the
594 nutrient uptake. Journal of Sea Research, 38, 195-212.
595 Beukema, J.J., Baretta-Bekker, J.G., 1995. European Regional Seas Ecosystem
596 Model (1990-1993). Netherlands Journal of Sea Research (special issue), 33(3-
597 4).
598 Blackford, J.C., 1997. An analysis of benthic biological dynamics in a North Sea
599 ecosystem model. Journal of Sea Research, 38, 213-230.
600 Blackford, J.C., Burkill, P.H., 2002. Planktonic community structure and carbon
601 cycling in the Arabian Sea as a result of monsoonal forcing: the application of a
602 generic model. Journal of Marine System, 36, 239-267.

603 Blackford, J.C., Allen, J.I., Gilbert, F.J., 2004. Ecosystem dynamics at six
604 contrasting sites: a generic modelling study. Journal of Marine Systems, 52, 191-
605 215.
606 Bocci, M., Coffaro, G., Bendoricchio, G., 1997. Modelling biomass and nutrient
607 dynamics in eelgrass (*Zostera marina* L.): applications to the lagoon of Venice
608 (Italy) and Oresun (Denmark). Ecological Modelling, 102, 67-80.
609 Bolding, K., Burchard, H., Polhmann, T., Stips, A., 2002. Turbulence mixing in
610 the Northern Sea: a numerical model study. Continental Shelf Research, 22,
611 2707-2724.
612 Borowitzka, M.A., Lavery, P.S., van Keulen, M., 2006. Epiphytes of seagrasses.
613 In: Larkum, A.W.D., Orth, R.J., Duarte, C.M., (eds.), Seagrasses: biology,
614 ecology and conservation. Springer, Netherlands, pp. 441-461.
615 Burd, A.B., Dunton, K.H., 2001. Field verification of a light-driven model biomass
616 changes in the seagrass *Halodule wrightii*. Marine Ecology Progress Series, 209,
617 85-98.
618 Cabello-Pasini, A., Muñiz-Salazar, R., Ward, D.H., 2003. Annual variations of
619 biomass and photosynthesis in *Zostera marina* at its southern end of distribution
620 in the North Pacific. Aquatic Botany, 76, 31-47.
621 Canuto, V.M., Howard, A., Cheng, Y., Dubovikov, M.S., 2001. Ocean turbulence:
622 Part I. One-point closure model. Momentum and heat vertical diffusivities.
623 Journal Physical Oceanography, 31, 1413-1426.
624 Camacho-Ibar, V.F., Hernández-Ayón, J.M., Santamaría-del-Angel, E., Daesslé-
625 Heuser, L.W., Zertuche González, J.A., 2007. Relación de las surgencias con los

626 stocks de carbono en Bahía San Quintín, una laguna costera del NW de México.
627 In: Hernández-de-la-Torre, B., Gaxiola-Castro, G. (eds.), Carbono en
628 Ecosistemas Acuáticos de México. INE, CICESE, pp. 355-370.
629 Dennison, W.C., Alberte, R.S., 1982. Photosynthetic responses of *Zostera*
630 *marina* L. (eelgrass) to in situ manipulations of light intensity. Oecologia, 55, 137-
631 144.
632 Dixon, B.R., 2004. Interactions of seagrass beds and the water column: effects of
633 bed size and hydrodynamics. PhD Thesis. University of Maryland, USA.
634 Droop, M.R., 1973. Some thoughts on nutrient limitation in algae. Journal of
635 Phycology, 9, 264-272.
636 Duarte, C.M., Marba, N., Krause-Jensen, D., Sanchez-Camacho, M., 2007.
637 Testing predictive power of seagrass depth limit models. Estuaries and Coasts,
638 30, 652-656.
639 Ebenhöh, W., Baretta-Bekker, J.G., Baretta, J.W., 1997. The primary production
640 module in the marine ecosystem model ERSEM II, with emphasis on the light
641 forcing. Journal of Sea Research, 38, 173-193.
642 Ebenhöh, W., Kohlmeier, C., Radford, P.J., 1995. The benthic biological
643 submodel in the European Regional Seas Ecosystem Model. Netherlands
644 Journal of Sea Research, 33(3/4), 423-452.
645 Flores-Vidal, X., 2006. Circulación residual en Bahía San Quintín, B.C., México.
646 Tesis de Maestría en Ciencias, CICESE, Ensenada, México.

García-Esquivel, Z., González-Gómez, M.A., Ley-Lou, F., Mejía-Trejo, A., 2004. Potencial ostrícola del brazo oeste de Bahía San Quintín: Biomasa actual y estimación preliminar de la capacidad de carga. Ciencias Marinas, 30, 61-74.

Guimaraens, M.A., Moraes, A.P., Coutinho, R., 2005. Modeling *Ulva spp.* Dynamics in a tropical upwelling region. Ecological Modelling, 188, 448-460.

Ibarra-Obando, S.E., Solana-Arellano, E., Poumian-Tapia, M., 2007. El papel de *Zostera marina* en el ciclo del carbono en Bahía San Quintín, Baja California. In: Hernández-de-la-Torre, B., Gaxiola-Castro, G. (eds.), Carbono en Ecosistemas Acuáticos de México. INE, CICESE, pp. 201-213.

Jorgensen, P., Ibarra-Obando, S.E., Carriquiry, J.D., 2007. Top-down and bottom-up stabilizing mechanisms in eelgrass meadows differentially affected by coastal upwelling. Marine Ecology Progress Series, 333, 81–93.

Kaldy, J.E., Lee, K.S., 2007. Factors controlling *Zostera marina* L. growth in the eastern and western Pacific Ocean: comparisons between Korea and Oregon, USA. Aquatic Botanic, 87, 116-126.

Kjerfve, B., (ed). 1994. Coastal lagoon processes. Elsevier. Amsterdam, Netherlands, 577 pp.

Lara-Lara, J.R., Álvarez-Borrego, S., and Small, L.F., 1980. Variability and tidal exchange of ecological properties in a coastal lagoon. Journal Estuaries Coastal Marine Science, 11, 613-637.

Largier, J.L., Hollibaugh, J.T., and Smith, S.V., 1997. Seasonally hypersaline estuaries in Mediterranean-climate regions. Estuarine, Coastal and Shelf Science, 45, 789-797.

670 Lee, K.S., Dunton, K.H., 2000. Effects of nitrogen enrichment on biomass
671 allocation, growth, and leaf morphology of the seagrass *Thalassia testidium*.
672 Marine Ecology Progress Series, 44, 1204-1215.
673 Millán-Nuñez, R., Álvarez-Borrego, S., Nelson, D.M., 1982. Effects of physical
674 phenomena on the distribution of nutrients and phytoplankton productivity in a
675 coastal lagoon. Estuarine Coastal and Shelf Science, 15, 317-335.
676 Pauly, D., Yañez-Arancibia, A., 1994. Fisheries in coastal lagoons. In: Kjerfve, B.
677 (ed.). Coastal Lagoon Processes. Elsevier, Amsterdan, The Netherlands, pp.
678 377-400.
679 Pennington, T., J., Chavez, F.P., 2000. Seasonal fluctuations of temperature,
680 salinity, nitrate, chlorophyll and primary production at station H3/M1 over 1989-
681 1996 in Monterey Bay, California. Deep-Sea Research II, 47, 947-973.
682 Petihakis, G., Triantafyllou, G., Koutsoubas, D., Allen, I., Dounas, C., 1999.
683 Modelling the annual cycles of nutrients and phytoplankton in a Mediterranean
684 lagoon (Gialova, Greece). Marine Environmental Research, 48, 37-58.
685 Plus, M., Chapelle, A., Ménesguen, A., Deslous-Paoli, J.M., Auby, I., 2003.
686 Modelling seasonal dynamics of biomasses and nitrogen contents in a seagrass
687 meadow (*Zostera noltii* Hornem.): application to the Thau lagoon (French
688 Mediterranean coast). Ecological Modelling, 161, 213-238.
689 Poumian-Tapia, M., Ibarra-Obando, S.E., 1999. Demography and biomass of the
690 seagrass *Zostera marina* in a Mexican coastal lagoon. Estuaries, 22, 879-889.
691 Ralph, P.J., Tomasko, D., Moore, K., Seddon, S., Macinnis-Ng, C.M.O., 2006.
692 Human Impacts on seagrasses: eutrophication, sedimentation, and

693 contamination. In: Larkum, A.W.D, Orth, R.J., Duarte, C.M. (eds.), Seagrasses:
694 biology, ecology and conservation. Springer, The Netherlands, pp. 567-593.
695 Ruardij, P., van Raaphorst, W.V., 1995. Benthic nutrient regeneration in the
696 ERSEM ecosystem model of the North Sea. Netherlands Journal of Sea
697 Research, 33, 453-483
698 Solidoro, C., Pecenik, G., Pastres, R., Franco, D., Dejak, C., 1997. Modelling
699 macroalgae (*Ulva rigida*) in the Venice lagoon: model structure identification and
700 first parameters estimation. Ecological Modelling, 94, 191-206.
701 Torres, R., Allen, J.I., Figueiras, F.G., 2006. Sequential data assimilation in an
702 upwelling influenced estuary. Journal of Marine Systems, 60, 317-329.
703 Trancoso, A.R., Saraiva, S., Fernandes, L., Pina, P., Leitao, P., Neves, R., 2005.
704 Modelling macroalgae using a 3D hydrodynamic-ecological model in a shallow,
705 temperate estuary. Ecological Modelling, 187, 232-246.
706 Tyler, A.C., McGlathery, K.J., Anderson, I.C., 2001. Macroalgae mediation of
707 dissolved organic nitrogen fluxes in a temperate coastal lagoon. Estuarine
708 Coastal and Shelf Science, 53, 155-168.
709 Umlauf, L., Burchard, H., 2005. Second-order turbulence closure models for
710 geophysical boundary layers. A review of recent work. Continental Shelf
711 Research, 25, 795-827.
712 Vichi, M., Pinardi, N., Zavatarelli, M., Matteuci, G., Marcaccio, M., Bergamini,
713 M.C., Frascari, F., 1998. One dimensional ecosystem model results in the Po
714 prodelta area (northern Adriatic Sea). Environmental Modelling and Software 13,
715 471-481.

716 Ward, D.H., Morton, A., Tibbitts T.L., Douglas, D.C., Carrera-Gonzalez, E., 2003.
717 Long-term change in eelgrass distribution at Bahia San Quintin, Baja California,
718 Mexico, using satellite imagery. Estuaries, 26, 1529-1539.
719 Zimmerman, R.C., Smith, R.D., Alberte, R.S., 1987. Is growth of eelgrass
720 nitrogen limited? A numerical simulation of the effects of light and nitrogen on the
721 growth dynamics of *Zostera. marina*. Marine Ecology Progress Series, 41, 167-
722 176.
723
724
725
726
727
728
729
730
731
732
733
734
735
736
737
738

## Figure captions

Figure 1. Map of San Quintin Bay showing the station of simulation (8), the sampling stations (6 and 10) used for calculation of the nutrient concentration gradients, the sampling stations and the location of the ADCP mooring. The –45˚ angle indicates the orientation of the channel in which station E8 is located, and is the angle for which ADCP data were rotated.

Figure 2. Biological and physical interactions between the components used in the coupled model GOTM-ERSEM (General Ocean Turbulence Model-European Regional Seas Ecosystem Model).

Figure 3. Observed meteorological data during 2004 used to force the physical model. Daily observations for the whole year are shown for air temperature, atmospheric pressure and irradiance, and daily observations for May to July (the strong upwelling) are shown for wind velocity.

Figure 4. Nutrient concentration gradients (solid line) used to simulate the seasonal horizontal advection of nutrients through GOTM. Observed gradients calculated with field data (dots) show increased nitrate gradients (stronger advection) and increased short term variability (due to intensification-relaxing alternation) during the upwelling intensification season (April to July).

Figure 5. Nutrient concentrations computed with the model, with and without advection, and without *Ulva spp*.. Dots indicate field data.

Figure 6. Model results, with and without nutrient advection, of *Z. marina, Ulva spp.* and diatom biomasses.

762 Figure 7. Results of the sensitivity analysis obtained by varying PAR, by ±30%
763 around its nominal value, in the *Z. marina* and *Ulva spp*. modules.
764 Figure 8. Results of the sensitivity analysis obtained by varying the light limitation
765 factor, by ±30% around its nominal value, in the *Z. marina* and *Ulva spp*.
766 modules.
767 Figure 9. Results of the sensitivity analysis obtained by varying the maximum
768 uptake rate of nitrate, by ±30% around its nominal value, in the *Z. marina* and
769 *Ulva spp.* modules.

**Tables**

Table 1. Symbols and description of the state variables in the model.

| Variable | Description | Dimension |
|---|---|---|
| P | Phosphate | mmol P $m^{-3}$ |
| N (3) | Nitrate | mmol N $m^{-3}$ |
| N (4) | Ammonium | mmol N $m^{-3}$ |
| Si | Silicate | mmol Si $m^{-3}$ |
| Ri(1) | Dissolved organic matter | mg C $m^{-3}$, mmol N-P $m^{-3}$ |
| Ri(6) | Particulate organic matter | mg C $m^{-3}$, mmol N-P $m^{-3}$ |
| O(2) | Dissolved oxygen | mg C $m^{-3}$ |
| O(3) | Carbon dioxide | mg C $m^{-3}$ |
| P1,P2,P3 | Diatoms, Flagellates, Nanoplankton | mg C $m^{-3}$, mmol N-P-Si $m^{-3}$ |
| B1 | Pelagic Bacteria | mg C $m^{-3}$, mmol N-P $m^{-3}$ |
| Z4,Z5 | Mesozooplankton, Microzooplankton | mg C $m^{-3}$, mmol N-P $m^{-3}$ |
| H1,H2 | Bacteria aerobic, Bacteria anaerobic | mg C $m^{-3}$, mmol N-P $m^{-3}$ |
| Y2,Y3,Y4 | Deposit feeders, Suspension feeders | mg C $m^{-3}$, mmol N-P $m^{-3}$ |
| Y5 | Meiobenthos, Benthic carnivores | |
| S1,S2 | *Z. marina* (leaf, roots) | mg C $m^{-3}$, mmol N-P $m^{-3}$ |
| U | *Ulva spp*. | mg C $m^{-3}$, mmol N-P $m^{-3}$ |

**Tables**

Table 2. Parameters for the seagrass module.

| | Symbol | Unit | Value |
|---|---|---|---|
| Maximal growth leaf | $\mu_{max}S1$ | $d^{-1}$ | 0.08 |
| Maximal growth roots | $\mu_{max}S2$ | $d^{-1}$ | 0.04 |
| q10 value temperature | *q10* | ---- | 2.00 |
| Basal respiration leaf | *rrestS1* | $d^{-1}$ | 0.01 |
| Basal respiration roots | *rrestS2* | $d^{-1}$ | 0.0005 |
| Activity respiration leaf | *ractS1* | ---- | 0.001 |
| Activity respiration roots | *ractS2* | ---- | 0.0005 |
| Exudation leaf | *Pu_eaS1* | $d^{-1}$ | 0.10 |
| Exudation roots | *Pu_eaS2* | $d^{-1}$ | 0.004 |
| Minimal N:C ratio | *Nmin* | mmol N:mmol C | 0.006 |
| Maximum N:C ratio | *Nmax* | mmol N:mmol C | 0.05 |
| Minimal P:C ratio | *Pmin* | mmol P:mmol C | 0.00042 |
| Maximum P:C ratio | *Pmax* | mmol P:mmol C | 0.00078 |
| Uptake rate of N3 | *VmS1n3* | mg (g Dw)$^{-1}$ $h^{-1}$ | 0.06 |
| Uptake rate of N4 | *VmS1n4* | mg (g Dw)$^{-1}$ $h^{-1}$ | 0.3 |
| Uptake rate of P | *VmS1P* | mg (g Dw)$^{-1}$ $h^{-1}$ | 0.05 |
| Uptake rate of N4 | *VmS2n4* | mg (g Dw)$^{-1}$ $h^{-1}$ | 0.83 |
| Half constant nitrate leaf | *KS1n3* | ---- | 2.00 |
| Half constant ammonium roots | *KS2n4* | ---- | 0.50 |
| Half constant phosphorus leaf | *KS1P* | ---- | 2.00 |
| Half constant phosphorus roots | *KS2P* | ---- | 0.50 |
| Mortality constant leaf | *Pu_daS1* | $d^{-1}$ | 0.01 |
| Mortality constant roots | *Pu_daS2* | $d^{-1}$ | 0.005 |
| Active radiation coefficient | *fPAR* | ---- | 0.50 |

**Tables**

Table 3. Parameters for the macroalga module.

| Parameter | Symbol | Unit | Value |
|---|---|---|---|
| Maximal growth | $\mu_{max}$ | $d^{-1}$ | 0.25 |
| q10 value temperature | *q10* | ---- | 2.00 |
| Basal respiration | *rrestU* | $d^{-1}$ | 0.001 |
| Activity respiration | *ractU* | ---- | 0.030 |
| Exudation | *Pu_eaU* | $d^{-1}$ | 0.200 |
| Minimal N:C ratio | *Nmin* | mmol N:mmol C | 0.0012 |
| Maximum N:C ratio | *Nmax* | mmol N:mmol C | 0.090 |
| Minimal P:C ratio | *Pmin* | mmol P:mmol C | 0.00087 |
| Maximum P:C ratio | *Pmax* | mmol P:mmol C | 0.00031 |
| Uptake rate of N3 | *VmUn3* | mg $(g\ Dw)^{-1}\ h^{-1}$ | 0.7 |
| Uptake rate of N4 | *VmUn4* | mg $(g\ Dw)^{-1}\ h^{-1}$ | 2.0 |
| Uptake rate of P | *VmUP* | mg $(g\ Dw)^{-1}\ h^{-1}$ | 0.23 |
| Half constant nitrate | *KUn3* | ---- | 2.00 |
| Half constant phosphorus | *KUP* | ---- | 0.323 |
| Mortality constant | *Pu_daU* | $d^{-1}$ | 0.009 |
| Active radiation coefficient | *fPAR* | ---- | 0.50 |

**Figure**

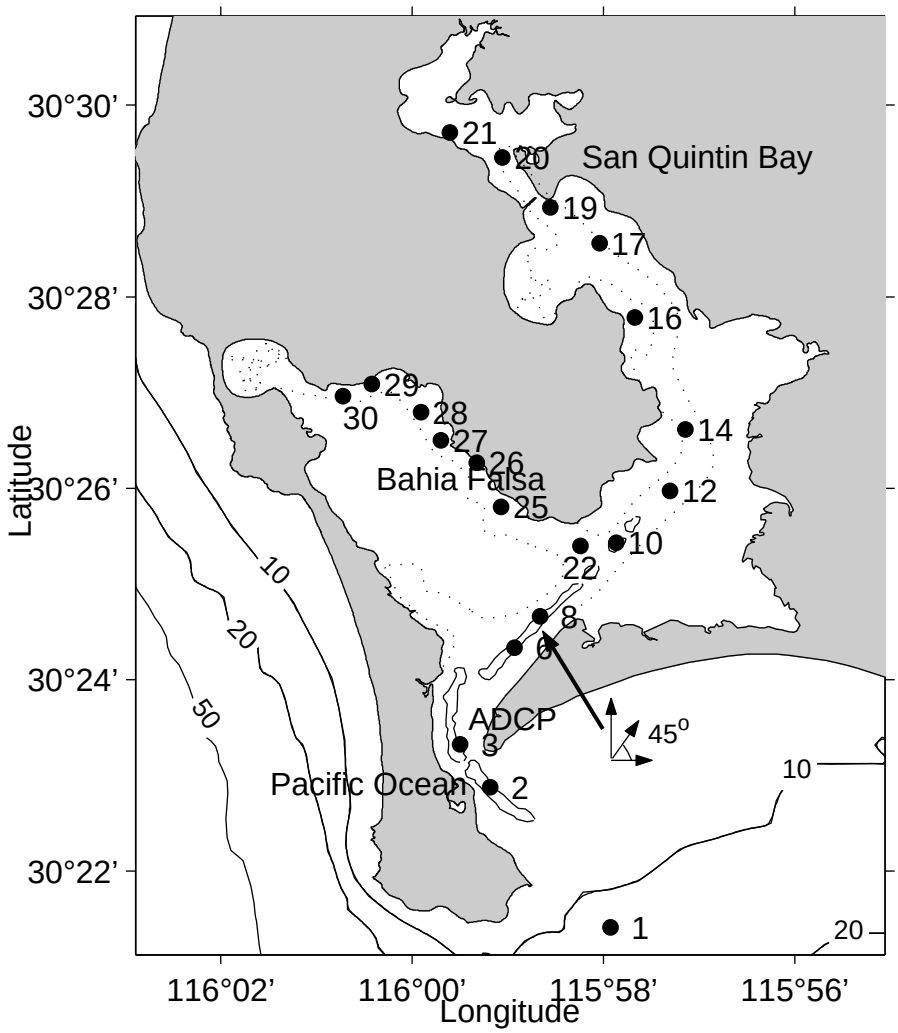
30°30’
30°28’
30°26’
30°24’
30°22’
Latitude
116°02’
116°00’
115°58’
115°56’
Longitude
San Quintin Bay
Bahia Falsa
Pacific Ocean
ADCP
45°
10
20
50
21
20
19
17
16
29
30
28
27
26
25
14
12
10
22
8
6
3
2
1

Figure

Click here to download high resolution image

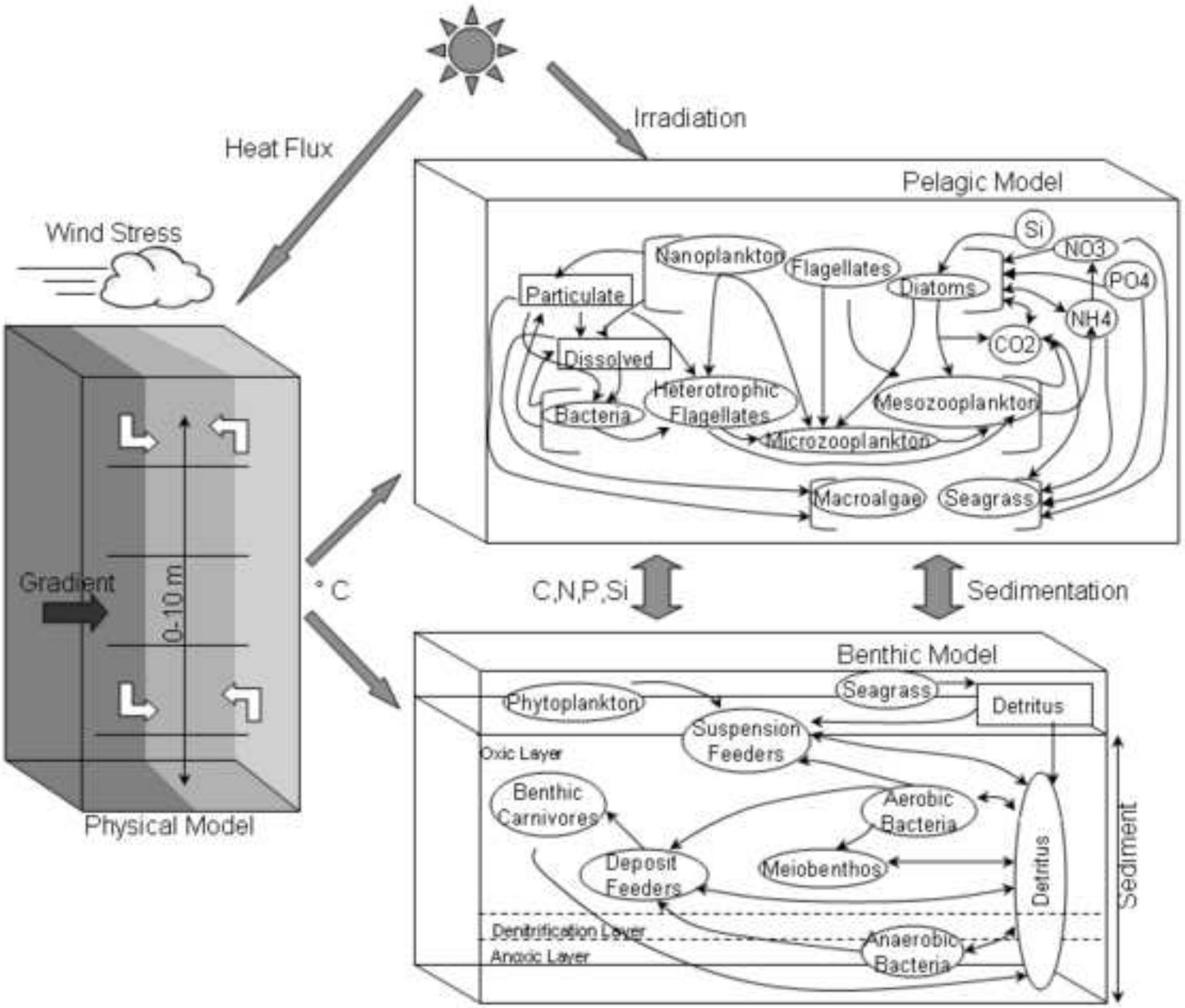

**Figure**

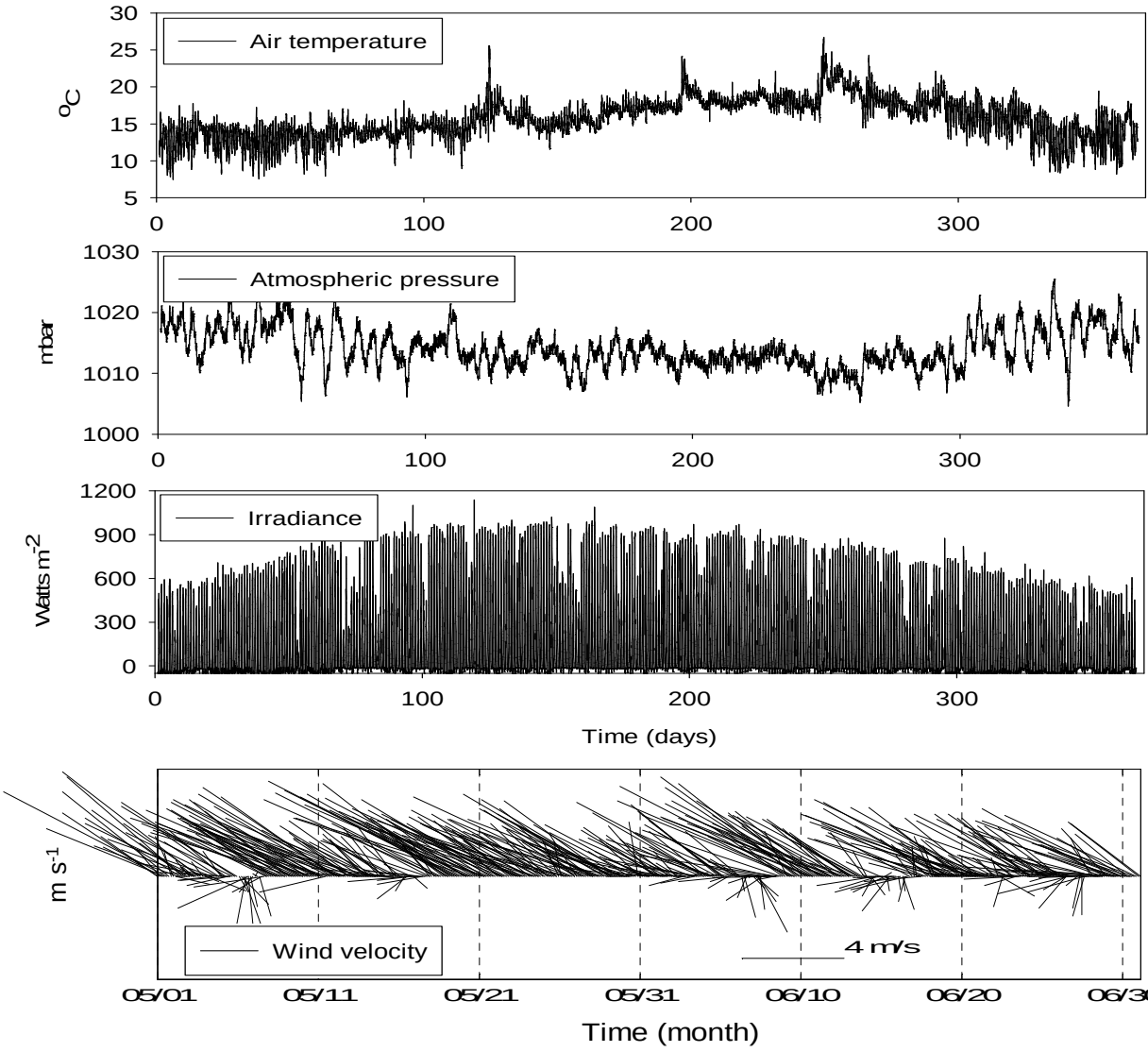


Figure 3

**Figure**

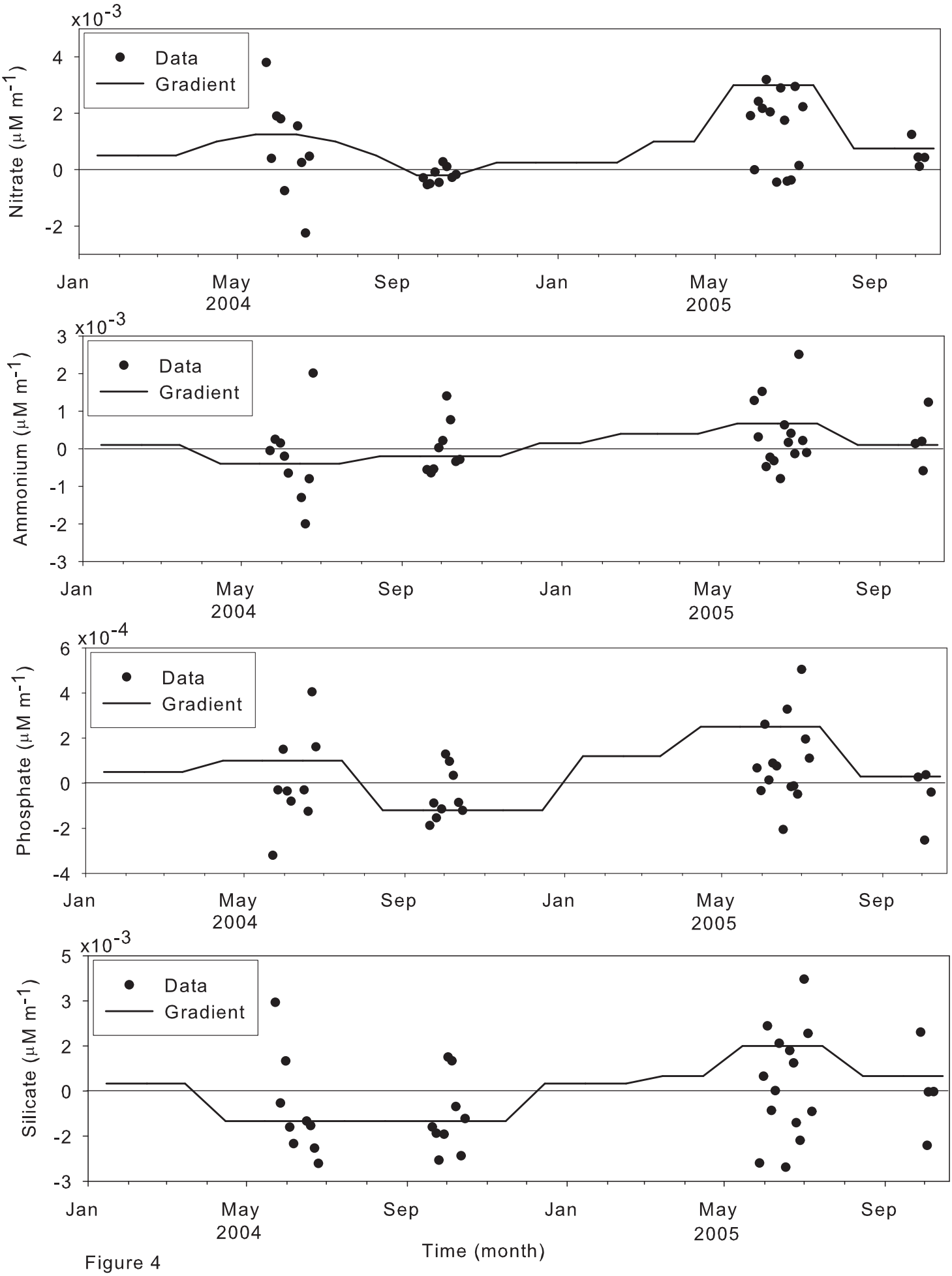


Figure 4

**Figure**

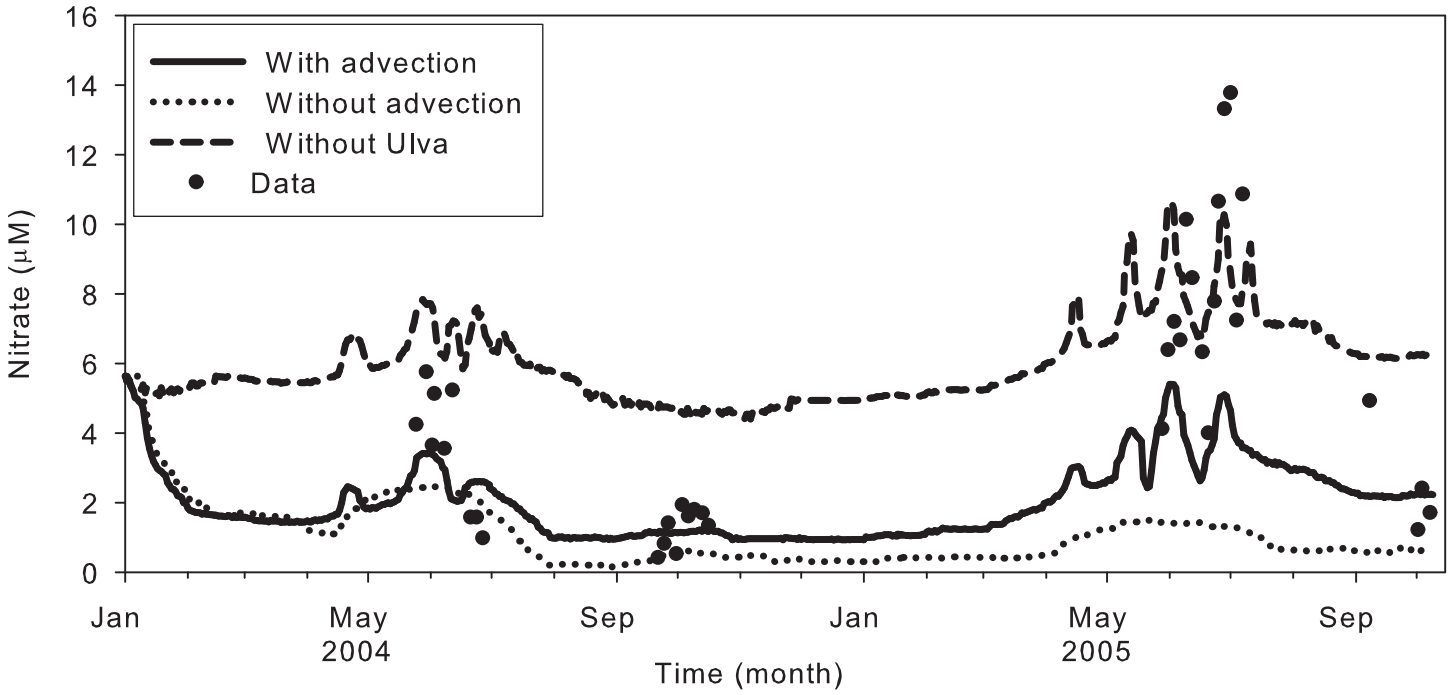


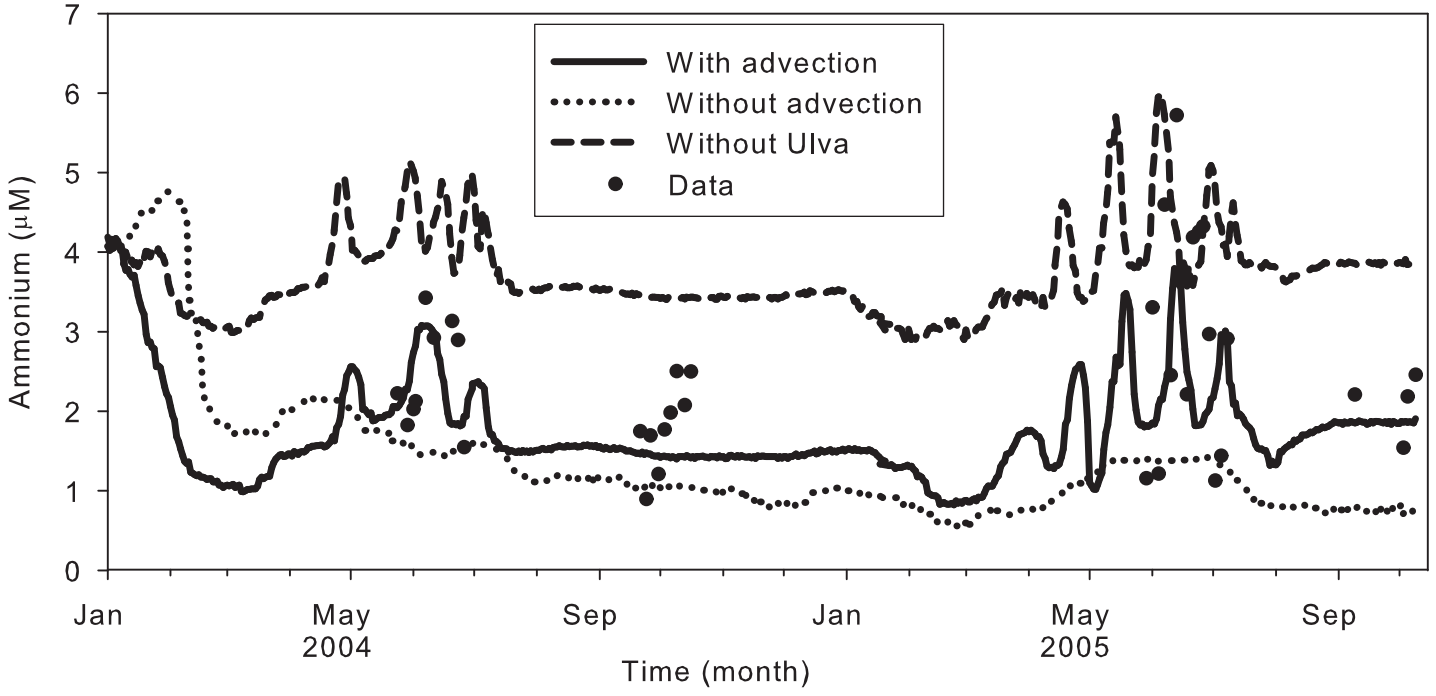


Figure 5

**Figure**

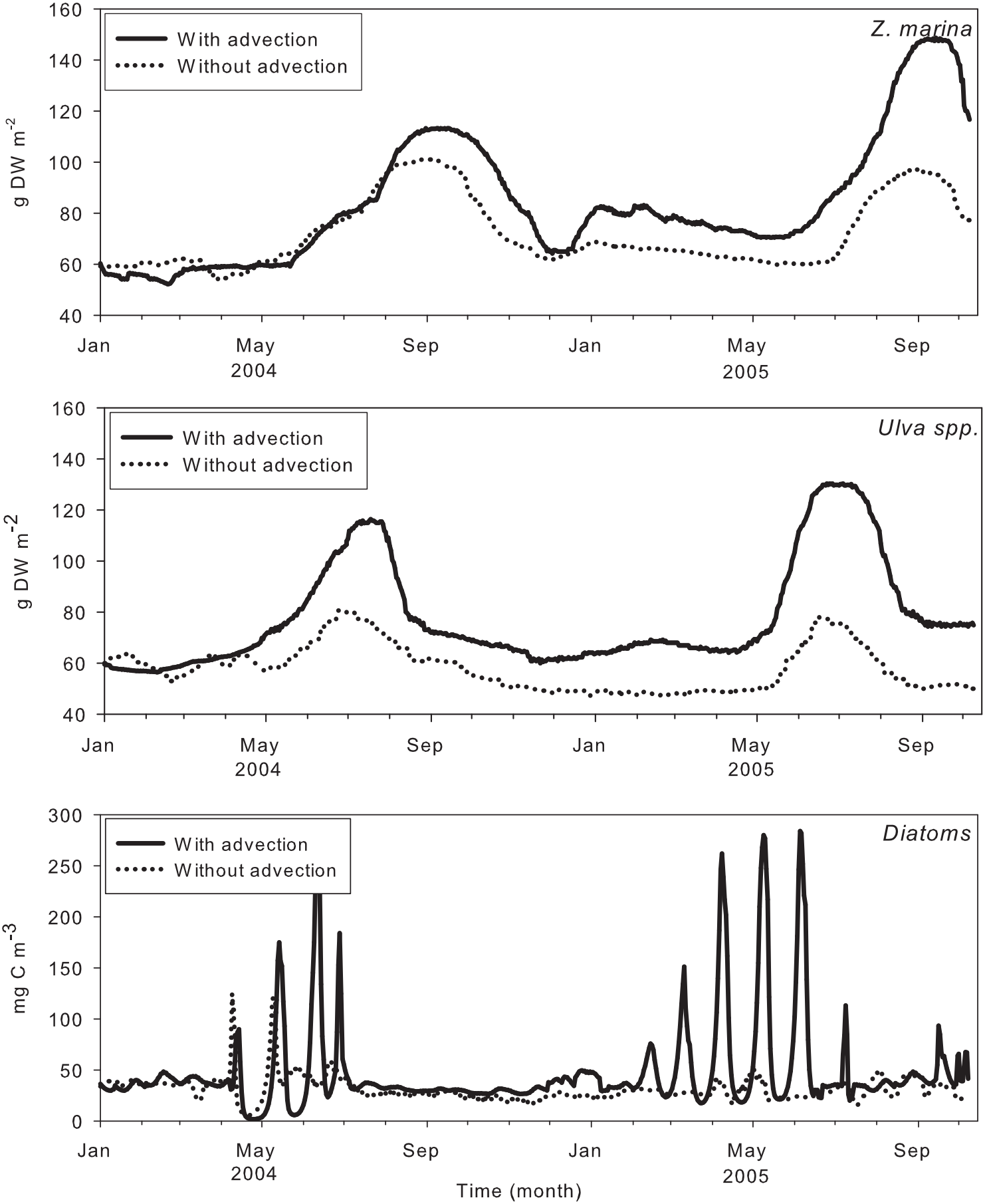


Figure 6

**Figure**

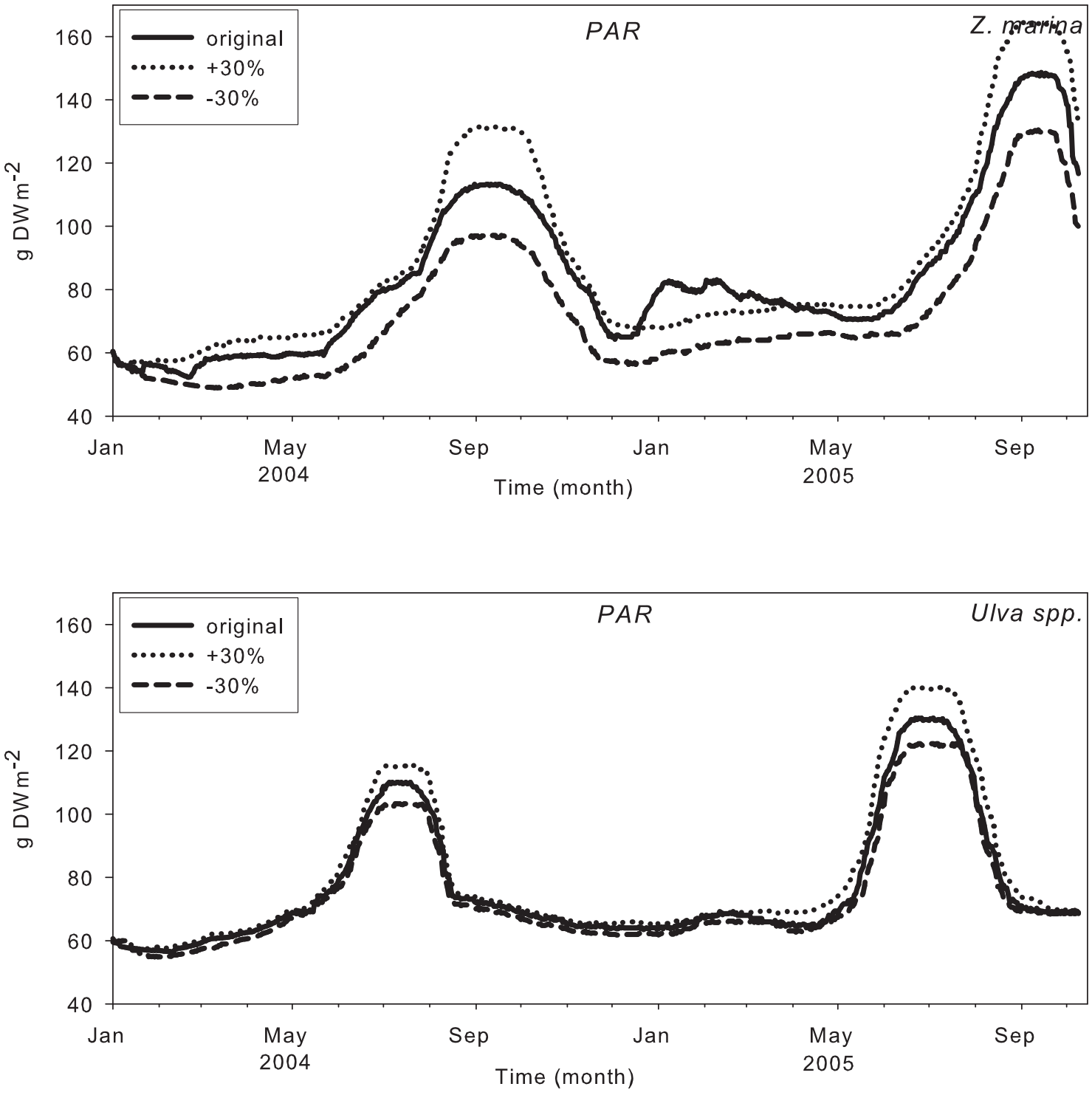


Figure 7

**Figure**

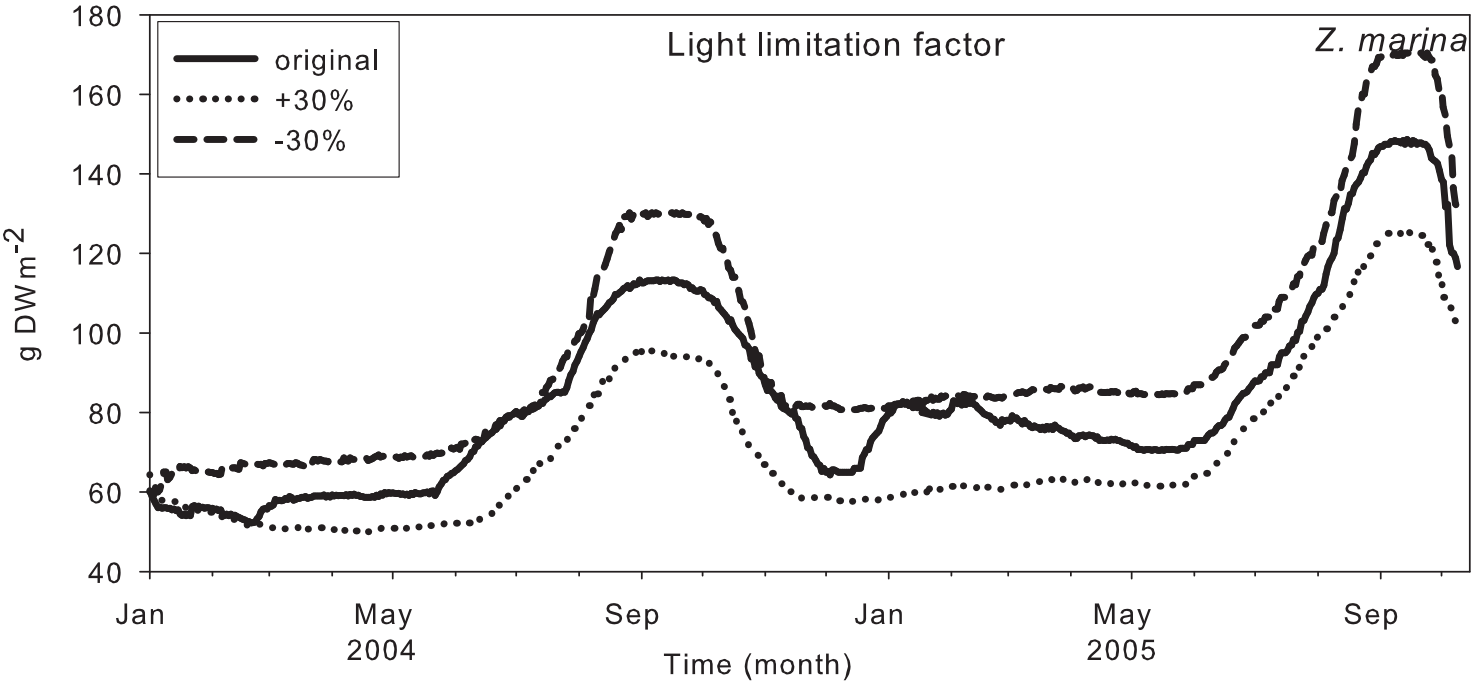


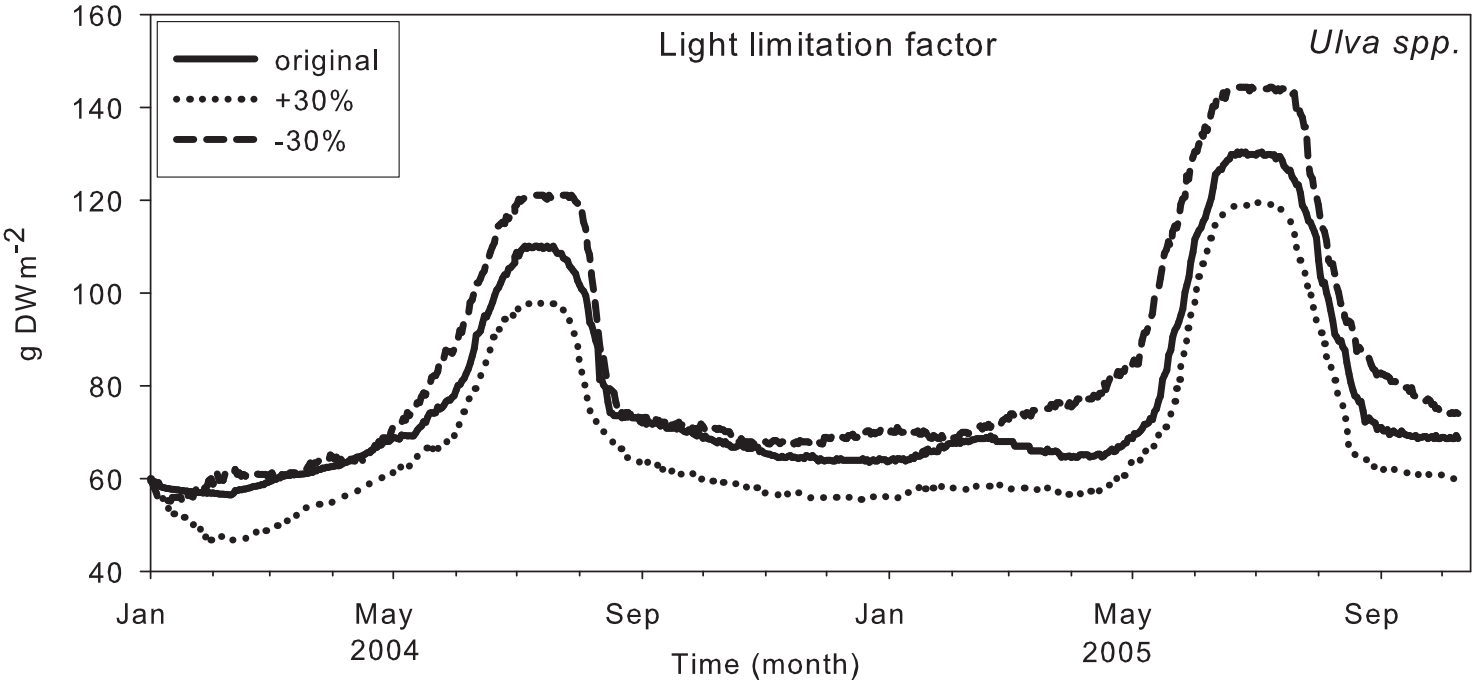


Figure 8

**Figure**

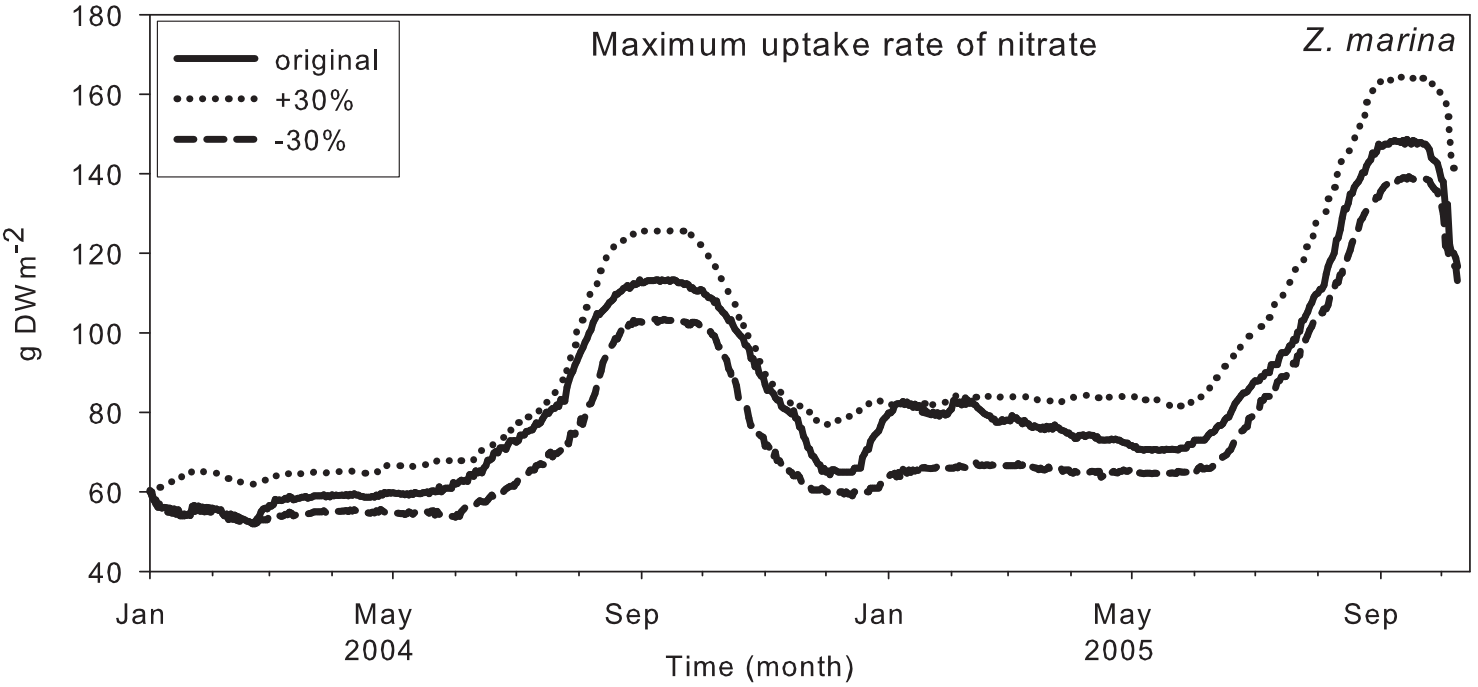


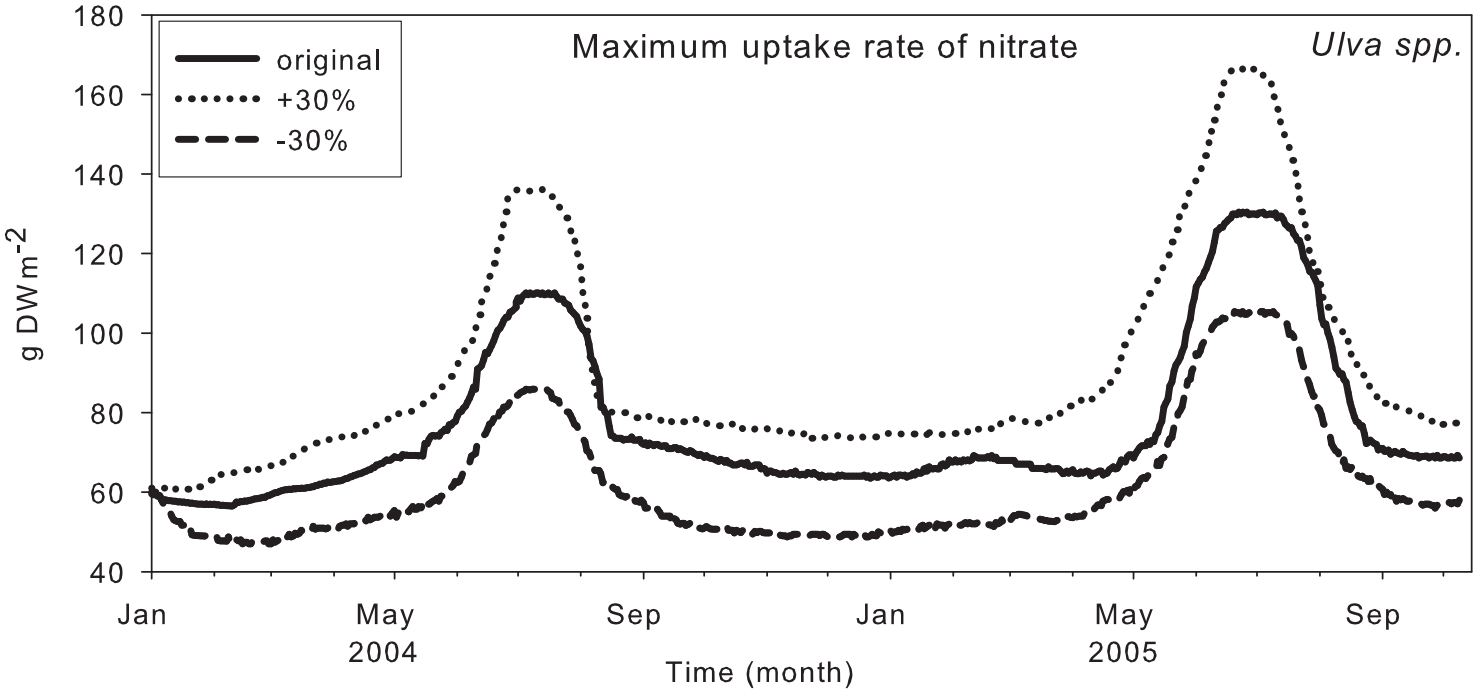


Figure 9